Automatica 142 (2022) 110255

Contents lists available at ScienceDirect

Automatica

journal homepage: www.elsevier.com/locate/automatica

Brief paper

A spatio-temporal reference trajectory planner approach to collision-free continuum deformation coordination ☆

Hossein Rastgoftar [a,*], Ilya V. Kolmanovsky [b]

[a] Department of Aerospace and Mechanical Engineering, University of Arizona, Tucson, AZ, 85721, USA
[b] Department of Aerospace Engineering, University of Michigan, Ann Arbor, MI, 48109, USA

ARTICLE INFO

Article history:
Received 29 October 2020
Received in revised form 14 November 2021
Accepted 13 January 2022
Available online xxxx

Keywords:
Multi-agent systems
Continuum deformation
And decentralized control
Optimization
Search methods

ABSTRACT

This paper proposes a spatio-temporal reference trajectory planner approach to safely plan continuum deformation coordination of a multi-agent system (MAS) in an obstacle-laden environment. We formulate a desired n-D continuum deformation as a leader–follower problem guided by $n+1$ leaders and followed by the remaining follower agents either through direct communication with leaders or communication with neighboring agents. To plan a safe continuum deformation coordination, we first provide sufficient conditions for inter-agent and obstacle collision avoidance. Then, we spatially optimize the continuum deformation coordination using the A* search to determine leaders' desired waypoints in an obstacle-laden environment. Leaders' desired waypoints are connected through C^1 continuous paths that are assigned by the spline curve fitting method. The desired trajectories of the leaders are then determined by planning a piece-wise constant reference input such that travel time is minimized and safety of the continuum deformation coordination is ensured.

1. Introduction

Multi-agent coordination has been extensively studied over the past two decades. Cooperative and formation control can enhance robustness of multi-agents systems (MASs) to mission failure and minimize the mission cost. Formation flight (Li & Liu, 2008), surveillance (Remagnino, Tan, & Baker, 1998), multi-agent coverage (Zhai & Hong, 2013), save and rescue (Al Tair, Taha, Al-Qutayri, & Dias, 2015), and cooperative payload transport (Klausen, Fossen, Johansen, & Aguiar, 2015) are some existing applications of multi-agent coordination.

Consensus (Li et al., 2018; Lin & Zheng, 2016; Liu, Cheng, Tan, & Hou, 2018; Zhou, Sang, Li, Fang, & Wang, 2018), containment control (Liu, Cheng, Tan, & Hou, 2015), and continuum deformation (Rastgoftar, Atkins, & Kolmanovsky, 2021; Rastgoftar & Kolmanovsky, 2021) are some of the existing multi-agent system (MAS) coordination methods. The delayed multi-agent consensus problems (Zhou et al., 2018), and finite-time consensus under fixed and switching communication topologies (Li et al., 2018; Lin & Zheng, 2016; Liu et al., 2018) have also been addressed. More recently, conditions for resilient consensus problem and for reaching consensus in the presence of anomalous/deceptive/failure agents (Dibaji & Ishii, 2017; Shang, 2018) have been developed. Containment control is a decentralized leader–follower multi-agent coordination approach in which leaders independently lead collective motion and followers infer the desired group coordination via communication with their in-neighbors. Containment control of a multi-agent system under fixed (Li, Chen, Liu, Zhang, & Zhang, 2016) and switching (Liu et al., 2015) communication topologies have been analyzed. Retarded containment with fixed (Li et al., 2016) and time-varying (Zhao, He, Saberi Nik, & Ren, 2015) time-delays and finite-time containment control and coordination (Zhao & Duan, 2015) have also been investigated. Wang and Wang (2019) provide necessary and sufficient conditions for stability of discrete-time containment control in the absence and presence of time delays. In continuum deformation coordination methods agents are treated as particles of a deformable body (or continuum) and their coordination is achieved by exploiting a continuum deformation function (Rastgoftar & Kolmanovsky, 2021). Similar to containment control, continuum deformation is a decentralized leader–follower approach, leaders guide the collective motion, and followers communicate with their in-neighbors to learn the desired coordination through local communication (Rastgoftar et al., 2021; Rastgoftar & Kolmanovsky, 2021). While the stability and convergence of the MAS to the convex hull defined by leader agents has been studied in the containment control literature (Ji,

☆ This work has been supported by the National Science Foundation under Award Nos. 2133690 and 1914581. The material in this paper was not presented at any conference. This paper was recommended for publication in revised form by Associate Editor Vijay Gupta under the direction of Editor Christos G. Cassandras.

* Corresponding author.
E-mail addresses: hrastgoftar@arizona.edu (H. Rastgoftar), ilya@umich.edu (I.V. Kolmanovsky).

https://doi.org/10.1016/j.automatica.2022.110255
0005-1098/

Ferrari-Trecate, Egerstedt, & Buffa, 2008; Wang & Wang, 2019), the proposed continuum deformation approach formally characterizes the deviation from the desired continuum deformation coordination and ensures that followers always remain inside the n-D leading simplex, defined by the leader agents by constraining the lower and upper bounds of the eigenvalues of the Jacobian matrix involved into the continuum deformation coordination.

In the existing literature (De Badyn, Eren, Açikmeşe, & Mesbahi, 2018), the MAS coordination is often approached in a setting of an optimal mass transport where the mass density transformation is assigned as the solution of a constrained optimal control problem. In this paper, MAS is represented by a finite number of particles of a deformable body (or continuum) and the optimization of continuum deformation is interpreted as a variant of a reference governor problem by defining a trajectory optimization problem for formation leaders and by decomposing it into spatial and temporal planning (optimization) problems. For the spatial optimization problem, A* search method (Rastgoftar et al., 2021; Rastgoftar & Kolmanovsky, 2021; Tseng, Liang, Lee, Der Chou, & Chao, 2014) is applied to assign optimal configurations of the leader agents by minimizing the travel distance between the initial and target configurations of the MAS. For every leader agent, the optimal path is then defined by a $\mathcal{C}^1$ continuous polynomial function connecting every two consecutive way-points, assigned by the A* planner. For the temporal optimization, we first define the leaders' desired trajectories based on a piece-wise constant reference input. Then, the reference input is planned such that optimal leaders' trajectories minimize the travel time between the way points and satisfy all safety constraints (i.e., ensure agent containment with no inter-agent or obstacle collisions). Compared to the existing literature and the authors' previous work (Rastgoftar et al., 2021), we propose an approach to speed up the computations of collision-free continuum deformation coordination by removing the previously needed requirement to bring the formation to rest at each waypoint. Furthermore, this paper provides sufficient safety conditions for continuum deformation coordination of a heterogeneous agent team with different sizes and characteristics.

The problem statement is presented in Section 2 and is followed by the derivation of the MAS collective and error dynamics in Section 3. The proposed approach to continuum deformation coordination planning is addressed in Section 4. Simulation results are presented in Section 5 and followed by the discussion and conclusions in Section 6.

2. Preliminaries and problem formulation

We consider an MAS consisting of N agents moving collectively in a 3-D space where every agent is uniquely identified by an index number $i \in \mathcal{V} = \{1, \ldots, N\}$. By classifying agents as leaders and followers, $\mathcal{V}$ can be expressed as $\mathcal{V} = \mathcal{V}_L \bigcup \mathcal{V}_F$, where $\mathcal{V}_L = \{1, \ldots, n+1\}$ and $\mathcal{V}_F = \mathcal{V} \setminus \mathcal{V}_L$ define the leaders' and followers' index numbers, respectively, in an n-D affine transformation where $n \in \{1, 2, 3\}$. Inter-agent communication is defined by digraph $\mathcal{G}(\mathcal{V}, \mathcal{E})$ with node set $\mathcal{V}$ and edge set $\mathcal{E} \subset \mathcal{V} \times \mathcal{V}$. Given an edge set $\mathcal{E}$, in-neighbor agents of agent $i \in \mathcal{V}$ are defined by $\mathcal{N}_i = \{j \in \mathcal{V} | (j, i) \in \mathcal{E}\}$. Note that leaders move independently, therefore $\mathcal{N}_i = \emptyset$, if $i \in \mathcal{V}_L$.

The dynamics of each of N agents $i \in \mathcal{V}$ is modeled by

$$\begin{cases} \dot{\mathbf{x}}_i = \mathbf{f}_i(\mathbf{x}_i) + \mathbf{g}_i(\mathbf{x}_i)\mathbf{u}_i \\ \mathbf{r}_i = \mathbf{C}_i \mathbf{x}_i \end{cases} \tag{1}$$

with state $\mathbf{x}_i \in \mathbb{R}^{n_{x,i}\times 1}$, input $\mathbf{u}_i \in \mathbb{R}^{n_{u,i}\times 1}$, and output $\mathbf{r}_i \in \mathbb{R}^{n\times 1}$. Here, $\mathbf{C}_i \in \mathbb{R}^{n\times n_{x,i}}$, $\mathbf{r}_i$ is the actual position of agent $i \in \mathcal{V}$, and $\mathbf{f}_i : \mathbb{R}^{n_{x,i}} \to \mathbb{R}^{n_{x,i}}$ and $\mathbf{g}_i : \mathbb{R}^{n_{x,i}} \to \mathbb{R}^{n_{x,i}\times n_{u,i}}$ are smooth functions.

We assume that the dynamics of every agent $i \in \mathcal{V}$ is feedback-linearizable; with state transformation $\mathbf{x}_i \to (\mathbf{y}_i, \varpi_i)$, the model (1) is converted to

$$\dot{\mathbf{y}}_i = \begin{bmatrix} \mathbf{0}_{n(\rho-1)\times n} & \mathbf{I}_{n(\rho-1)} \\ \mathbf{0}_{n\times n} & \mathbf{0}_{n\times n(\rho-1)} \end{bmatrix} \mathbf{y}_i + \begin{bmatrix} \mathbf{0}_{n(\rho-1)\times n} \\ \mathbf{I}_n \end{bmatrix} \mathbf{s}_i \tag{2}$$

$$\dot{\varpi}_i = \mathbf{h}(\varpi_i, \mathbf{y}_i, \mathbf{s}_i), \tag{3}$$

where $\mathbf{h}(\varpi_i, \mathbf{y}_i, \mathbf{s}_i)$ is smooth, and $\mathbf{y}_i = \left[\mathbf{r}_i^T \quad \cdots \quad \left(\frac{d^{\rho-1}\mathbf{r}_i}{dt^{\rho-1}}\right)^T\right]^T$.

For every agent $i \in \mathcal{V}$, we define a global desired position $\mathbf{r}_{i,HT}(t)$ over the time interval $[t_{init}, t_f]$ with fixed initial time t_{init} and final time t_f, by *homogeneous transformation* that is given by

$$\mathbf{r}_{i,HT}(t) = \mathbf{Q}(t)\mathbf{r}_{i,0} + \mathbf{d}(t), \qquad \forall i \in \mathcal{V}, \tag{4}$$

where $\mathbf{Q}(t) \in \mathbb{R}^{n\times n}$ is a non-singular Jacobian matrix, $\mathbf{d}(t) \in \mathbb{R}^n$ is the rigid-body displacement vector at time t, and $\mathbf{r}_{i,0}$ is the reference position of agente $i \in \mathcal{V}$. Each agent $i \in \mathcal{V}$ is controlled to stably track the desired trajectory

$$\mathbf{r}_{i,d}(t) = \begin{cases} \mathbf{r}_{i,HT} & i \in \mathcal{V}_L \\ \sum_{j\in\mathcal{N}_i} w_{i,j}\mathbf{r}_j & \forall i \in \mathcal{V}_F \end{cases}, \qquad \forall t \in [t_0, t_f] \tag{5}$$

by choosing

$$\mathbf{s}_i = \sum_{h=0}^{\rho-1} \gamma_{i,h} \frac{d^h(\mathbf{r}_{i,d} - \mathbf{r}_i)}{dt^h}, \tag{6}$$

where $\gamma_{i,1}$ through $\gamma_{i,\rho-1}$ are constant control gains and $w_{i,j} > 0$ is the communication weight between agent $i \in \mathcal{V}$ and the in-neighbor agent $j \in \mathcal{N}_i$. Given control gains $\gamma_{i,1}$ through $\gamma_{i,\rho-1}$, we define gain matrix

$$\mathbf{G}_h = \mathbf{diag}(\gamma_{1,h}, \ldots, \gamma_{N,h}), \qquad h = 0, \ldots, \rho-1. \tag{7}$$

Then the model for the external dynamics of the MAS is obtained as follows (Rastgoftar, 2020):

$$\begin{aligned} \frac{d^\rho \mathbf{Y}(t)}{dt^\rho} = &\sum_{h=0}^{\rho-1} \left(\mathbf{I}_\rho \otimes (\mathbf{G}_h(-\mathbf{I} + \mathbf{L}))\right) \frac{d^h(\mathbf{Y}_d(t) - \mathbf{Y}(t))}{dt^h} \\ &+ \sum_{h=0}^{\rho-1} \left(\mathbf{I}_\rho \otimes (\mathbf{G}_h\mathbf{L}_0)\right) \frac{d^h\mathbf{R}_L(t)}{dt^h}, \end{aligned} \tag{8}$$

where $\mathbf{L}_0 = \begin{bmatrix}\mathbf{I}_{n+1} & \mathbf{0}\end{bmatrix}^T \in \mathbb{R}^{N\times(n+1)}$ while the matrix $\mathbf{L} = [L_{ij}] \in \mathbb{R}^{N\times N}$ and vectors $\mathbf{R}_L(t) \in \mathbb{R}^{n(n+1)\times 1}$, $\mathbf{Y}_d(t) \in \mathbb{R}^{nN\times 1}$, and $\mathbf{Y}(t) \in \mathbb{R}^{nN\times 1}$, aggregating components of the global desired positions of leaders, reference desired positions of all agents, and actual positions of all agents, respectively, are defined as follows:

$$L_{ij} = \begin{cases} w_{i,j} & i \in \mathcal{V}_F \wedge j \in \mathcal{N}_i \\ 0 & \text{otherwise.} \end{cases} \tag{9a}$$

$$\mathbf{R}_L(t) = \mathrm{vec}\left(\begin{bmatrix}\mathbf{r}_{1,HT}(t) & \cdots & \mathbf{r}_{n+1,HT}(t)\end{bmatrix}^T\right), \qquad \forall t \in [t_{init}, t_f], \tag{9b}$$

$$\mathbf{Y}_d(t) = \mathrm{vec}\left(\begin{bmatrix}\mathbf{r}_{1,d}(t) & \cdots & \mathbf{r}_{N,d}(t)\end{bmatrix}^T\right), \forall t \in [t_{init}, t_f], \tag{9c}$$

$$\mathbf{Y}(t) = \mathrm{vec}\left(\begin{bmatrix}\mathbf{r}_1(t) & \cdots & \mathbf{r}_N(t)\end{bmatrix}^T\right), \forall t \in [t_{init}, t_f], \tag{9d}$$

where "vec" is the matrix vectorization symbol.

The main objective of this paper is to develop a method for planning a safe continuum deformation by prescribing the vector $\mathbf{R}_L(t)$ over a finite time interval. To this end, we define

$$\mathbf{R}_L(t) = \mathbf{P}_k\begin{bmatrix}(\eta(t) - \eta(t_k))^3 & \cdots & \eta(t) - \eta(t_k) & 1\end{bmatrix}^T \tag{10}$$

for $t \in [t_k, t_{k+1})$ and $k = 1, \ldots, n_w$, where $\mathbf{P}_k \in \mathbb{R}^{n(n+1)\times 4}$ is the kth shape matrix that remains constant over $[t_k, t_{k+1})$, and the evolution of the generalized coordinate η is defined as follows:

$$\dot{\eta}(t) = v_k, \qquad t \in [t_k, t_{k+1}), \tag{11}$$

subject to conditions

$$\eta(t_k) = k, \qquad k = 1, \ldots, n_w - 1, \tag{12a}$$

$$\eta(t_{k+1}) = k + 1, \qquad k = 1, \ldots, n_w - 1, \tag{12b}$$

where v_k is constant over the time-interval $[t_k, t_{k+1})$. Thus, $v_k = \frac{1}{T_k}$ is constant at any time $t \in [t_k, t_{k+1})$ for $k = 1, \ldots, n_w - 1$, where $T_k = t_{k+1} - t_k$. As a result, $\mathbf{R}_L(t)$, can be written as follows:

$$\mathbf{R}_L(t) = \mathbf{P}_k \begin{bmatrix} \left(\frac{t-t_k}{T_k}\right)^3 & \left(\frac{t-t_k}{T_k}\right)^2 & \frac{t-t_k}{T_k} & 1 \end{bmatrix}^T \tag{13}$$

Given the above problem setting, continuum deformation planning is decomposed into spatial and temporal optimization problems. For the spatial optimization, we determine leaders' intermediate waypoints by minimizing the travel distance between the leaders' initial and final configurations. Then, the shape matrix $\mathbf{P}_k$ is assigned using the spline method such that leaders' desired paths are defined by $\mathcal{C}^1$ continuous polynomial connecting consecutive leaders' way-points. For the temporal optimization, we solve the following problem:

$$\left(T_1^*, \ldots, T_{n_w-1}^*\right) = \underset{v_1,\ldots,v_{n_w-1}}{\arg\min} \sum_{k=1}^{n_w-1} T_k \tag{14}$$

such that

$$\forall t, \qquad \bigwedge_{i\in\mathcal{V}} \left(\|\mathbf{r}_i(t) - \mathbf{r}_{i,HT}(t)\| \le \delta_i\right), \tag{15a}$$

$$\forall t,\ \forall i, j \in \mathcal{V},\ i \ne j, \qquad \|\mathbf{r}_i(t) - \mathbf{r}_j(t)\| \ge \epsilon_i + \epsilon_j \tag{15b}$$

$$\forall t, \qquad \bigwedge_{i\in\mathcal{V}} \left(\mathbf{r}_i(t) \in \mathcal{B}(t)\right), \tag{15c}$$

where $T_k = t_{k+1} - t_k$ ($k = 1, \ldots, n_w - 1$), and δ_i is an upper-bound on the deviation of every agent $i \in \mathcal{V}$ from global desired position $\mathbf{r}_{i,HT}(t)$, defined by Eq. (4) at time t, and

$$\mathcal{B}(t) = \{\mathbf{r} : \|\mathbf{r} - \mathbf{d}(t)\| \le r_{\max}\} \tag{16}$$

is the rigid containment ball with radius $r_{\max}$ which is centered at $\mathbf{d}(t)$ at any time t.

Although, we assume that dynamics of every agent $i \in \mathcal{V}$ is deterministic, the deviation upper-bound δ_i can account for model uncertainty and control errors when planning a large-scale continuum deformation coordination. Let ϵ_i and ϵ_j be the radii of the smallest rigid balls enclosing agents i and j ($i \ne j$), then constraint equation (15b) ensures the inter-agent collision avoidance for every two different agents at any time t. The above optimization problem is computationally-expensive and the computation cost is large, if n_w is large. To reduce the computation cost, we impose the following condition:

$$k = 1, \ldots, n_w - 1, \qquad \bigwedge_{i\in\mathcal{V}} \left(\left\| \frac{d^j\mathbf{r}_i(t_k)}{dt^j} - \frac{d^j\mathbf{r}_{i,HT}(t_k)}{dt^j} \right\| \le \beta_j\delta_i\right), \tag{17}$$

for $0 < \beta_j < 1$ ($j = 1, \ldots, \rho$). Then we can plan continuum deformation by solving the following independent optimization problems:

$$k = 1, \ldots, n_w - 1, \qquad \min_{v_k} T_k \tag{18}$$

subject to constraint equations (15a), (15b), (15c), and (17) for $t_k \le t < t_{k+1}$.

In what follows, we first obtain the MAS collective dynamics and assign the coordination error (Section 3). Then, Section 4 addresses planning of a safe plan continuum deformation coordination using the above spatio-temporal reference trajectory planner approach.

3. MAS collective dynamics

Given $\mathbf{R}_L(t)$, defined by Eq. (13), the time derivatives of $\mathbf{R}_L(t)$ are obtained as

$$j = 1, \ldots, \rho - 1, \qquad \frac{d^j\mathbf{R}_L}{dt^j} = \sum_{h=j}^{3} \frac{(h)!}{(h-j)!}\mathbf{p}_{h,k}(t - t_k)^{h-j}. \tag{19}$$

where

$$\begin{bmatrix}\mathbf{p}_{3,k} & \cdots & \mathbf{p}_{0,k}\end{bmatrix} = \mathbf{P}_k \mathrm{diag}\left(\frac{1}{T_k^3}, \frac{1}{T_k^2}, \frac{1}{T_k}, 1\right). \tag{20}$$

Substituting $\mathbf{R}_L(t), \cdots, \frac{d^{\rho-1}\mathbf{R}_L}{dt^{\rho-1}}(t)$ into Eq. (8), the MAS collective dynamics becomes

$$t \in [t_k, t_{k+1}), \qquad \dot{\mathbf{X}}_{\mathrm{MAS}}(t) = \mathbf{A}_{\mathrm{MAS}}\mathbf{X}_{\mathrm{MAS}}(t) + \sum_{h=0}^{3}(t - t_k)^h \mathbf{c}_{h,k}, \tag{21}$$

where

$$\mathbf{X}_{\mathrm{MAS}}(t) = \begin{bmatrix}\mathbf{Y}^T(t) & \cdots & \left(\frac{d^{\rho-1}\mathbf{Y}(t)}{dt^{\rho-1}}\right)^T\end{bmatrix}^T \in \mathbb{R}^{n\rho N\times 1}, \tag{22a}$$

$$\mathbf{A}_{\mathrm{MAS}} = \begin{bmatrix} \mathbf{0}_{nN} & \mathbf{I}_{nN} & \cdots & \mathbf{0}_{nN} \\ \vdots & \vdots & \ddots & \vdots \\ \mathbf{0}_{nN} & \mathbf{0}_{nN} & \cdots & \mathbf{I}_{nN} \\ \mathbf{I}_n \otimes (\mathbf{G}_0(-\mathbf{I}_N + \mathbf{L})) & \mathbf{I}_n \otimes (\mathbf{G}_1(-\mathbf{I}_N + \mathbf{L})) & \cdots & \mathbf{I}_n \otimes (\mathbf{G}_{\rho-1}(-\mathbf{I}_N + \mathbf{L})) \end{bmatrix}, \tag{22b}$$

$$\mathbf{c}_{h,k} = \sum_{j=0}^{3}\sum_{h=0}^{\zeta(j)} \frac{(h+j)!}{h!}\begin{bmatrix}\mathbf{0}_{n(\rho-1)N\times n(n+1)} \\ \mathbf{I}_n \otimes (\mathbf{G}_j\mathbf{L}_0)\end{bmatrix}\mathbf{p}_{h+j,k}, \tag{22c}$$

$$\zeta(j) = \min\{3, 3 - j\}. \tag{22d}$$

Theorem 1. *Define* $\mathbf{Y}_{HT}(t) = \mathrm{vec}\left(\begin{bmatrix}\mathbf{r}_{1,HT} & \cdots & \mathbf{r}_{N,HT}\end{bmatrix}^T\right)$, *and* $\mathbf{E} = \mathbf{Y} - \mathbf{Y}_H T$ *as the error vector, characterizing from theglobal desired positions. If* $\rho < 4$, *the error dynamics is given by*

$$t \in [t_k, t_{k+1}), \qquad \dot{\mathbf{Z}}(t) = \mathbf{A}_{\mathrm{MAS}}\mathbf{Z}(t) + \sum_{h=0}^{3}\mathbf{d}_{h,k}(t - t_k)^\rho \tag{23}$$

where $\mathbf{Z}(t) = \begin{bmatrix}\mathbf{E}^T(t) & \cdots & \left(\frac{d^{\rho-1}\mathbf{E}(t)}{dt^{\rho-1}}\right)^T\end{bmatrix}^T \in \mathbb{R}^{n\rho N\times 1}$ *and*

$$\mathbf{d}_{h,k} = \sum_{h=0}^{\zeta(\rho)} \frac{(h+\rho)!}{h!}\begin{bmatrix}\mathbf{0}_{9N\times n(n+1)} \\ \mathbf{I}_n \otimes (\mathbf{G}_\rho\mathbf{L}_0)\end{bmatrix}\mathbf{p}_{h+\rho,k} \tag{24}$$

for $k \in [t_k, t_{k+1})$ *and* $k = 1, \ldots, n_w - 1$.

Proof. Per Theorem 3 of Rastgoftar and Kolmanovsky (2021).

$$\mathbf{I}_n \otimes \left(\mathbf{G}_j(-\mathbf{I}_N + \mathbf{L})\frac{d^j\mathbf{Y}}{dt^j} + \mathbf{G}_j\mathbf{L}_0\frac{d^j\mathbf{R}_L}{dt^j}\right) = \mathbf{I}_n \otimes \left(\mathbf{G}_j(-\mathbf{I}_N + \mathbf{L})\frac{d^j\mathbf{E}}{dt^j}\right)$$

for $j = 1, \cdots, \rho$ and the error dynamics becomes

$$\dot{\mathbf{Z}}(t) = \mathbf{A}_{\text{MAS}}\mathbf{Z}(t) + \begin{bmatrix} \mathbf{0}_{n(\rho-1)N\times n(n+1)} \\ \mathbf{I}_n \otimes \left(\mathbf{G}_\rho \left(-\mathbf{I}_N + \mathbf{L}\right)^{-1}\mathbf{L}_0\right) \end{bmatrix} \frac{d^\rho \mathbf{R}_L}{dt^\rho} \tag{25}$$

for $t \in [t_k, t_{k+1})$. By substituting $\frac{d^\rho \mathbf{R}_L}{dt^\rho}$ from Eq. (19) in Eq. (25), Eq. (25) can be written in the form of Eq. (23) where $\mathbf{d}_{h,k}$ is given by (24). □

Per Theorem 1,

$$\mathbf{Z}(t) = \Phi(t, t_k)\mathbf{Z}_k + \sum_{h=0}^{\zeta(\rho)} \Theta_h(t, t_k)\mathbf{d}_{h,k}, \tag{26}$$

at $t \in [t_k, t_{k+1})$ where $\rho < 4$,

$$\Phi(t, t_k) = e^{\mathbf{A}_{\text{MAS}}(t-t_k)}, \tag{27a}$$

$$\Theta_h(t, t_k) = \int_{t_k}^{t} (\tau - t_k)^h e^{\mathbf{A}_{\text{MAS}}(\tau - t_k)} d\tau, \tag{27b}$$

and $\mathbf{Z}_k = \mathbf{Z}(t_k)$ for $k = 1, \ldots, n_w - 1$.

Remark 1. To characterize error, we can write

$$\left\| \frac{d^j \mathbf{r}_i}{dt^j} - \frac{d^j \mathbf{r}_{i,HT}}{dt^j} \right\|_2^2 = \mathbf{Z}^T(t)\mathbf{O}_{ij}^T\mathbf{O}_{ij}\mathbf{Z}(t) \tag{28}$$

where $\|\cdot\|_2$ denotes the 2-norm symbol, $j = 0, \ldots, \rho - 1$, $i \in \mathcal{V}$, $\mathbf{O}_{ij} = \left[O_{ij}{}_{lh}\right] \in \mathbb{R}^{n\times(nN\rho)}$, and the (l, h) element of matrix $\mathbf{O}_{ij}$ is defined as follows:

$$O_{ij}{}_{lh} = \begin{cases} 1 & \bigwedge_{l=1}^{n} (h = jNn + (l-1)N + i) \\ 0 & \text{otherwise.} \end{cases} \tag{29}$$

Note that $n \in \{1, 2, 3\}$ is the dimension of the homogeneous transformation coordination, $N = |\mathcal{V}|$ is the total number of agents, and ρ is the dimension of the feedback linearized dynamics (see Eq. (2)).

Remark 2. Note that positive control gains $\gamma_{1,1}, \cdots, \gamma_{\rho,1}, \cdots, \gamma_{1,N}, \cdots, \gamma_{\rho,N}$ are such that the matrix $\mathbf{A}_{\text{MAS}}$ is Hurwitz. As the result, the external dynamics of the MAS, given by (8), is BIBO stable.

Theorem 2. *Define*

$$\Phi_{\max,j} = \sqrt{\max_{t,\forall i\in\mathcal{V}} \mathbf{1}^T\Phi^T(t, 0)\mathbf{O}_{ij}^T\mathbf{O}_{ij}\Phi(t, 0)\mathbf{1}}.$$

for $j = 0, \ldots, \rho - 1$. Assume safety condition (17) is satisfied, $0 < \beta_j < 1$ for $j = 0, \ldots, \rho - 1$, and control gains $\gamma_{i,h}$ ($i \in \mathcal{V}$ and $h \in \{0, \ldots, \rho - 1\}$) are selected such that

$$\forall j \in \{0, \ldots, \rho - 1\}, \qquad \beta_j < \min_{\forall i\in\mathcal{V}} \left(\frac{\delta_i}{\Phi_{\max,j}}\right), \tag{30}$$

where $\mathbf{1}$ is the one-entry vector. Then, there exist travel times $T_1, \ldots, T_{n_w-1}$ such that safety condition (15a) and (17) are satisfied at any time $t \in [t_1, t_{n_w}]$ where $t_1 = t_{init}$ and $t_{n_w} = t_f$ are the initial and final time, respectively.

Proof. Because $\mathbf{A}_{\text{MAS}}$ is Hurwitz, $\Phi(t, t_k)$ and $\Theta(t, t_k)$, defined by (27), are bounded. Per Eqs. (24) and (20), $\mathbf{d}_{h,k} \to \mathbf{0}$, if $T_k \to \infty$. This implies that the second term on the right-hand side of Eq. (26) converges to $\mathbf{0}$, if $T_k \to \infty$. Therefore, safety condition (15a) can be satisfied, if

$$\bigwedge_{i,j,k} \left(\mathbf{Z}_k^T\Phi^T(t, t_k)\mathbf{O}_{ij}^T\mathbf{O}_{ij}\Phi(t, t_k)\mathbf{Z}_k < \delta_i^2\right), \qquad \forall t \in [t_k, t_{k+1}). \tag{31}$$

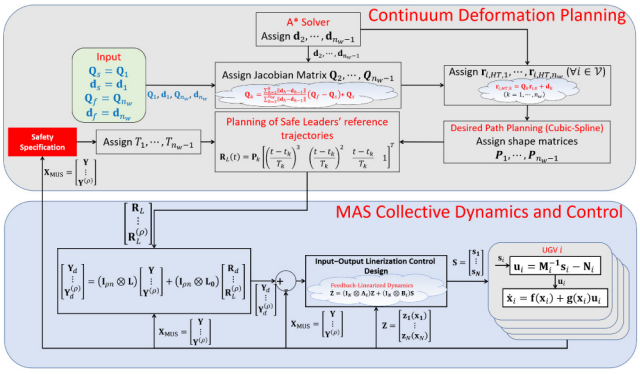

Fig. 1. Functionality of the continuum deformation guidance.

If (17) is satisfied, then,

$$\bigwedge_{i,j,k} \left(\mathbf{Z}_k^T\Phi^T(t, t_k)\mathbf{O}_{ij}^T\mathbf{O}_{ij}\Phi(t, t_k)\mathbf{Z}_k < \beta_j^2\mathbf{1}^T\Phi(t, t_k)\mathbf{O}_{ij}^T\mathbf{O}_{ij}\Phi(t, t_k)\mathbf{1}\right)$$

where

$$\bigwedge_{i,j,k} \left(\mathbf{1}^T\Phi^T(t, t_k)\mathbf{O}_{ij}^T\mathbf{O}_{ij}\Phi(t, t_k)\mathbf{1} \le \Phi_{\max,j}^2\right).$$

Hence, (31) is satisfied, if (30) holds. □

Theorem 2 assures safety by assigning an upper bound for β_j ($j = 0, \ldots, \rho - 1$) in a continuum deformation planning problem minimizing the cost function (18) and satisfying the constraints given in (15a) and (17).

4. Continuum deformation coordination planning

We propose a two-layer continuum deformation planning approach to ensure safety by defining leaders' desired trajectories at every time $t \in [t_{init}, t_f]$ (see Fig. 1). At the top level, the continuum deformation shape functions $\mathbf{P}_1$ through $\mathbf{P}_{n_w-1}$ are assigned through planning desired leaders' paths. At the low level, desired trajectories of leaders are assigned by planning the generalized coordinate η as the solution of optimization problem (18) subject to the constraints (15). This paper assumes that the geometry of the obstacles, the initial displacement vector $\mathbf{d}_1 = \mathbf{d}_{init} = \mathbf{d}(t_{init})$, the initial Jacobian matrix $\mathbf{Q}_1 = \mathbf{Q}_{init} = \mathbf{Q}(t_{init})$, the final displacement vector $\mathbf{d}_{n_w} = \mathbf{d}_f = \mathbf{d}(t_f)$, the final Jacobian matrix $\mathbf{Q}_{n_w} = \mathbf{Q}_f = \mathbf{Q}(t_f)$ are assumed to be known, where $t_f = t_{n_w}$ is free. Then, $\mathbf{d}_2, \ldots, \mathbf{d}_{n_w-1}$ and $\mathbf{Q}_2, \ldots, \mathbf{Q}_{n_w-1}$ are determined in Section 4.1.

4.1. High-level planning: Leader path planning

To plan leaders' desired paths, we first determine leaders' desired waypoints and then the leaders' desired paths are obtained using the cubic spline method.

4.1.1. Way-point planing

The desired way-points of leader $i \in \mathcal{V}_L$ are denoted by $\mathbf{r}_{i,HT,k} = \mathbf{r}_{i,HT}(t_k)$ and given by

$$\mathbf{r}_{i,HT,k} = \mathbf{Q}_k\mathbf{r}_{i,0} + \mathbf{d}_k,$$

where $\mathbf{Q}_k = \mathbf{Q}(t_k)$ and $\mathbf{d}_k = \mathbf{d}(t_k)$ are the Jacobian matrix and rigid-body displacement vector at time t_k ($k = 1, 2, \ldots, n_w - 1$). Therefore, the desired way-points of each leader $i \in \mathcal{V}_L$ are assigned at discrete time instants t_k by determining $\mathbf{d}_k$ and $\mathbf{Q}_k$ as described below.

4.1.1.1. Assignment of rigid-body displacement. The A* search (Tseng et al., 2014) is applied to determine desired way-points of the center of containment ball $\mathcal{B}$ by minimizing the travel distance between the initial position and target destination. To this end, we uniformly discretize the space and represent it by a finite number of characteristic nodes defined by set

$$\mathcal{D}=\left\{\tilde{\mathbf{d}}=\left(i_1\bar{\Delta},\ldots,i_n\bar{\Delta}\right):i_k\in\left\{i_{k,\min},\ldots,i_{k,\max}\right\},i_{k,\min},\right.$$
$$\left.i_{k,\max}\in\mathbb{Z},\ k=1,\ldots,n,\ \bar{\Delta}\in\mathbb{R}_{>0}\right\},$$

Obstacles defined by a set $\mathcal{M}\subset\mathcal{D}$ must be avoided by the containment ball. Therefore, the immediate in-neighbors of a characteristic node $\tilde{\mathbf{d}}\in\mathcal{D}\setminus\mathcal{M}$ form a set

$$\mathcal{I}\left(\tilde{\mathbf{d}}\right)=\left\{\tilde{\mathbf{d}}'\in\mathcal{D}\setminus\mathcal{M}:\|\tilde{\mathbf{d}}'-\tilde{\mathbf{d}}\|\leq\bar{\Delta}\mathbf{1}_{n\times1}\right\}. \tag{32}$$

For every $\tilde{\mathbf{d}}\in\mathcal{D}\setminus\mathcal{M}$ and $\tilde{\mathbf{d}}'\in\mathcal{I}\left(\tilde{\mathbf{d}}\right)$,

$$C_H\left(\tilde{\mathbf{d}},\mathbf{d}_f\right)=\|\tilde{\mathbf{d}}-\tilde{\mathbf{d}}_f\| \tag{33a}$$

$$C_O\left(\tilde{\mathbf{d}},\tilde{\mathbf{d}}'\right)=\|\tilde{\mathbf{d}}-\tilde{\mathbf{d}}'\| \tag{33b}$$

are defined as the heuristic cost and the operation cost for a given final destination $\mathbf{d}_f$.

Proposition 1. *By choosing $\bar{\Delta}>r_{\max}$, we can ensure that the containment ball does not collide with obstacles, if: (i) the MAS is always contained by the containment ball $\mathcal{B}$, and (ii) the center of the containment ball $\mathcal{B}$ moves along the line segment connecting $\tilde{\mathbf{d}}\in\mathcal{D}\setminus\mathcal{M}$ and $\tilde{\mathbf{d}}'\in\mathcal{I}\left(\tilde{\mathbf{d}}\right)$.*

Proof. If followers always remain inside the containment ball $\mathcal{B}$, and the containment ball $\mathcal{B}$ moves along the line segment connecting $\tilde{\mathbf{d}}\in\mathcal{D}\setminus\mathcal{M}$ and $\tilde{\mathbf{d}}'\in\mathcal{I}\left(\tilde{\mathbf{d}}\right)$, the minimum distance of the center of the containment ball from any obstacle node defined by $\mathcal{O}$ is $\bar{\Delta}$. If $r_{\max}<\bar{\Delta}$, then, no interior point of the containment ball can collide with obstacle nodes and hence collision avoidance is guaranteed. □

Per Proposition 1, our multi-agent path planning can be reduced to a way-point planning problem, where the intermediate way-points of the center of the containment ball, denoted by $\mathbf{d}_2$, $\cdots$, $\mathbf{d}_{n_w-1}$, are determined by Algorithm 1.

4.1.1.2. Assignment of Jacobian matrix. Given $\mathbf{d}_1$ through $\mathbf{d}_{n_w}$ assigned by the A* solver, $\mathbf{Q}_{init}$, and $\mathbf{Q}_f$, $\mathbf{Q}_k$ is interpolated by

$$\mathbf{Q}_k=(1-\mu_k)\,\mathbf{Q}_{init}+\mu_k\mathbf{Q}_f, \tag{34}$$

for $k=2,\ldots,n_w-1$, where $\mu_k=\dfrac{\sum_{h=2}^{k}\|\mathbf{d}_h-\mathbf{d}_{h-1}\|}{\sum_{h=2}^{n_w}\|\mathbf{d}_h-\mathbf{d}_{h-1}\|}\in[0,1]$.

4.1.2. Desired leaders' paths

The desired position of leader $i\in\mathcal{V}_L$ is defined by a third-order polynomial

$$k=0,\ldots,n_w,\ t\in[t_k,t_{k+1}),\qquad \mathbf{r}_{i,HT}(t)=\sum_{l=0}^{3}\mathbf{h}_{i,l,k}\,(t-t_k)^l$$

subject to $\mathbf{r}_{i,HT}(t_k^-)=\mathbf{r}_{i,HT}(t_k^+)$ and $\dot{\mathbf{r}}_{i,HT}(t_k^-)=\dot{\mathbf{r}}_{i,HT}(t_k^+)$ for $k=2,\ldots,n_w-1$. This paper uses the cubic spline method to determine $\mathbf{h}_{i,l,k}\in\mathbb{R}^{3\times1}$ for every $i\in\mathcal{V}_L$, $l=1,2,3$, and $k=0,1,\ldots,n_w-1$. Therefore, $\mathbf{R}_L(t)$ is defined as in Eq. (13) where

$$h=1,\ldots,3,\qquad \mathbf{p}_{h,k}=\mathrm{vec}\left(\begin{bmatrix}\mathbf{h}_{1,h,k} & \cdots & \mathbf{h}_{n+1,h,k}\end{bmatrix}^T\right).$$

Algorithm 1 A* Procedure for Optimal Planning of the Leaders' Paths

Get: $\mathbf{d}_1$, $\mathbf{d}_f$, *obstacle set* $\mathcal{M}$
Define: Open set $\mathcal{O}=\{\mathbf{d}_1\}$, Closed set $\mathcal{C}=\emptyset$, and $\tilde{\mathbf{d}}_{\text{best}}=\mathbf{d}_1$
while $\tilde{\mathbf{d}}_{\text{best}}\neq\mathbf{d}_f$ or $\mathcal{O}\neq\emptyset$ **do**
  $\tilde{\mathbf{d}}_{\text{best}}\leftarrow\underset{\tilde{\mathbf{d}}\in\mathcal{O}}{\text{argmin}}\left(g\left(\tilde{\mathbf{d}}\right)+C_H\left(\tilde{\mathbf{d}},\mathbf{d}_f\right)\right)$
  Update $\mathcal{O}$: $\mathcal{O}\leftarrow\mathcal{O}\setminus\left\{\tilde{\mathbf{d}}_{\text{best}}\right\}$ and $\mathcal{C}$: $\mathcal{C}\leftarrow\mathcal{C}\bigcup\left\{\tilde{\mathbf{d}}_{\text{best}}\right\}$
  Assign $\mathcal{I}\left(\tilde{\mathbf{d}}_{\text{best}}\right)$
  $\mathcal{R}\left(\tilde{\mathbf{d}}_{\text{best}}\right)\leftarrow\mathcal{I}\left(\tilde{\mathbf{d}}_{\text{best}}\right)\setminus\left(\mathcal{I}\left(\tilde{\mathbf{d}}_{\text{best}}\right)\bigcap\mathcal{C}\right)$
  for < `every` $\tilde{\mathbf{d}}\in\mathcal{R}\left(\tilde{\mathbf{d}}_{\text{best}}\right)$> **do**
    if $\tilde{\mathbf{d}}\in\mathcal{O}$ **then**
      if $g\left(\tilde{\mathbf{d}}_{\text{best}}\right)+C_O\left(\tilde{\mathbf{d}}_{\text{best}},\tilde{\mathbf{d}}\right)<g\left(\tilde{\mathbf{d}}\right)$ **then**
        $g\left(\tilde{\mathbf{d}}\right)\leftarrow g\left(\tilde{\mathbf{d}}_{\text{best}}\right)+C_O\left(\tilde{\mathbf{d}}_{\text{best}},\tilde{\mathbf{d}}\right)$
        $\tilde{\mathbf{b}}\left(\tilde{\mathbf{d}}\right)\leftarrow\tilde{\mathbf{d}}_{\text{best}}$
      end if
    end if
  end for
  $\mathcal{O}\leftarrow\mathcal{R}\left(\tilde{\mathbf{d}}_{\text{best}}\right)\bigcup\mathcal{O}$
end while

4.2. Trajectory planning

Given the leaders' desired paths, the shape matrix $\mathbf{P}_k$ is known over the time interval $[t_k,t_{k+1})$. Then, the optimal travel intervals T_1^* through $T_{n_w-1}^*$ are assigned by solving the optimization problem (18) subject to constraints (15).

It is computationally-expensive to ensure inter-agent collision avoidance and agent containment using constraint equations (15b) and (15c) when the total number of agents is large. In Lemma 1 and Theorem 3, we exploit the properties of the homogeneous deformation to reduce the computation cost by providing sufficient conditions for inter-agent and obstacle collision avoidance and agent containment.

Lemma 1. *Let every agent $i\in\mathcal{V}$ be enclosed by a ball of radius ϵ_i and the deviation of agent i from its global desired position be less than δ_i at any time t (safety condition (15a)). Then,*

$$\forall t,\ i,j\in\mathcal{V},\ i\neq j,\qquad \left|\|\mathbf{r}_i(t)-\mathbf{r}_j(t)\|-\left(\delta_i+\delta_j\right)\right|\leq\|\mathbf{r}_{i,HT}(t)-\mathbf{r}_{j,HT}(t)\|. \tag{35}$$

Also, inter-agent collision between two different agents i and j is to be avoided if

$$\forall t,\ i,j\in\mathcal{V},\ i\neq j,\qquad \|\mathbf{r}_{i,HT}(t)-\mathbf{r}_{j,HT}(t)\|\geq\epsilon_i+\delta_i+\epsilon_j+\delta_j. \tag{36}$$

Proof. Let $\mathbf{r}_i-\mathbf{r}_j=\left(\mathbf{r}_i-\mathbf{r}_{i,HT}\right)+\left(\mathbf{r}_{i,HT}-\mathbf{r}_{j,HT}\right)+\left(\mathbf{r}_{j,HT}-\mathbf{r}_j\right)$. Then,

$$\begin{aligned}\|\mathbf{r}_i-\mathbf{r}_j\|\leq&\|\mathbf{r}_i-\mathbf{r}_{i,HT}\|+\|\mathbf{r}_{i,HT}-\mathbf{r}_{j,HT}\|+\|\mathbf{r}_{j,HT}-\mathbf{r}_j\|\\ \leq&\delta_i+\|\mathbf{r}_{i,HT}-\mathbf{r}_{j,HT}\|+\delta_j.\end{aligned} \tag{37a}$$

$$\begin{aligned}\|\mathbf{r}_i-\mathbf{r}_j\|\geq&\|\mathbf{r}_i-\mathbf{r}_{i,HT}\|-\|\mathbf{r}_{i,HT}-\mathbf{r}_{j,HT}\|-\|\mathbf{r}_{j,HT}-\mathbf{r}_j\|\\ \geq&\|\mathbf{r}_{i,HT}-\mathbf{r}_{j,HT}\|-\delta_i-\delta_j.\end{aligned} \tag{37b}$$

Eq. (37b) implies that inter-agent collision avoidance condition, given in (15b), is satisfied, if $\|\mathbf{r}_{i,HT}-\mathbf{r}_{j,HT}\|\geq\epsilon_i+\delta_i+\epsilon_j+\delta_j$. □

Theorem 3. *Assume every agent can execute proper trajectory controller such that the safety condition (15a) is satisfied where the global desired position of every agent $i \in \mathcal{V}$ is defined by homogeneous transformation, given in (4), and $\sum_{i\in\mathcal{V}} \mathbf{r}_{i,0} = 0$. Inter-agent collision avoidance is guaranteed for $t \in [t_{init}, t_f]$, if*

$$i \in \{1, \dots, n\}, \qquad \lambda_i(t) \geq \lambda_{\min} \tag{38}$$

at any time $t \in [t_{init}, t_f]$ where $\lambda_i(t)$ is the ith eigenvalue of deformation matrix $\mathbf{U}_D(t) = \left(\mathbf{Q}^T(t)\mathbf{Q}(t)\right)^{\frac{1}{2}}$ and

$$\lambda_{\min} = \max_{i,j\in\mathcal{V},\ j\neq i} \frac{\delta_i + \epsilon_i + \delta_j + \epsilon_j}{\|\mathbf{r}_{i,0} - \mathbf{r}_{j,0}\|}. \tag{39}$$

Furthermore, agents are all located inside the containment ball $\mathcal{B}(t)$, defined by Eq. (16) if

$$i \in \{1, 2, 3\}, \qquad \lambda_i(t) \leq \lambda_{\max}, \qquad \forall t \in [t_{init}, t_f] \tag{40}$$

where

$$\lambda_{\max} = \min_{i\in\mathcal{V}} \frac{r_{\max} - \delta_i - \epsilon_i}{\|\mathbf{r}_{i,0}\|_2}. \tag{41}$$

Proof. Using Eq. (4), we can write

$$\|\mathbf{r}_{i,HT} - \mathbf{r}_{j,HT}\|_2^2 = \left(\mathbf{r}_{i,0} - \mathbf{r}_{j,0}\right)^T \mathbf{Q}^T\mathbf{Q}\left(\mathbf{r}_{i,0} - \mathbf{r}_{j,0}\right).$$

Thus,

$$\forall t \in [t_{init}, t_f], \qquad \lambda_{\min} \leq \frac{\|\mathbf{r}_{i,HT}(t) - \mathbf{r}_{j,HT}(t)\|_2}{\|\mathbf{r}_{i,0} - \mathbf{r}_{j,0}\|_2} \leq \lambda_{\max}$$

where $\lambda_{\min} = \min_{t\in[t_{init},t_f]}\{\lambda_1(t), \lambda_2(t), \lambda_3(t)\}$ and $\lambda_{\max} = \max_{t\in[t_{init},t_f]}\{\lambda_1(t), \lambda_2(t), \lambda_3(t)\}$. Inter-agent collision avoidance is guaranteed if

$$\min_{t\in[t_{init},t_f],\ i,j\in\mathcal{V},\ i\neq j} \left(\|\mathbf{r}_{i,HT}(t) - \mathbf{r}_{j,HT}(t)\|_2 - \epsilon_i - \delta_i - \epsilon_j - \delta_j\right) =$$

$$\min_{i,j\in\mathcal{V},\ i\neq j} \left(\lambda_{\min}\|\mathbf{r}_{i,0} - \mathbf{r}_{j,0}\|_2 - \epsilon_i - \delta_i - \epsilon_j - \delta_j\right) \geq 0.$$

Thus, $\lambda_{\min}$ is obtained by Eq. (39) and inter-agent collision avoidance is guaranteed, if Eq. (38) is satisfied at any time $t \in [t_{init}, t_f]$. Moreover, all agents remain inside the containment ball $\mathcal{B}(t)$, if

$$\max_{t\in[t_{init},t_f],\ i\in\mathcal{V}} \left(\|\mathbf{r}_{i,HT}(t) - \mathbf{d}(t)\|_2 + \epsilon_i + \delta_i\right) =$$

$$\max_{i\in\mathcal{V}} \left(\lambda_{\max}\|\mathbf{r}_{i,0}\|_2 + \epsilon_i + \delta_i\right) \leq r_{\max}.$$

This implies that $\lambda_{\max}$ is obtained by Eq. (41) and follower containment is assured if Eq. (40) is satisfied. □

Given the sufficient conditions provided by Theorem 3, a desired continuum deformation coordination is planned by solving the following constrained optimization problem:

$$k = 1, \dots, n_w - 1, \qquad \min T_k$$

subject to

$$\forall t \in [t_1, t_{n_w-1}], \qquad \mathbf{Z}(t) = \Phi(t, t_k)\mathbf{Z}_k + \sum_{h=0}^{\zeta(\rho)} \Theta_h(t, t_k)\mathbf{d}_{h,k} \tag{42a}$$

$$\forall t \in [t_1, t_{n_w-1}],\ \forall i \in \mathcal{V},\ j = 1, \dots, \rho, \qquad \mathbf{Z}^T(t)\mathbf{O}_{ij}^T\mathbf{O}_{ij}\mathbf{Z}(t) \leq \delta_i^2, \tag{42b}$$

$$k = 1, \dots, n_w,\ \forall i \in \mathcal{V},\ j = 1, \dots, \rho, \qquad \mathbf{Z}^T(t_k)\mathbf{O}_{ij}^T\mathbf{O}_{ij}\mathbf{Z}(t_k) \leq \beta_j^2\delta_i^2 \tag{42c}$$

$$\forall t \in [t_1, t_{n_w-1}],\ i = 1, 2, 3, \qquad \lambda_{\min} \leq \lambda_i(t) \leq \lambda_{\max}, \tag{42d}$$

where $\Phi(t, t_k)$, $\Theta_h(t, t_k)$, $\mathbf{O}_{ij}$, λ_{min}, and $\lambda_{\max}$ were previously defined, and $\lambda_i(t)$ is the ith eigenvalue of the deformation matrix $\mathbf{U}_D(t) = \left(\mathbf{Q}^T(t)\mathbf{Q}(t)\right)^{\frac{1}{2}}$.

5. Simulation results

We consider an MAS consisting of $N = 8$ UGVs, with the half-car dynamic model given in Rastgoftar, Zhang, and Atkins (2018). In this example, UGV team is identified by unique index numbers defined by set $\mathcal{V} = \{1, 2.\cdots, 8\}$ with leaders and followers defined by $\mathcal{V}_L = \{1, 2, 3\}$ and $\mathcal{V}_F = \{4, \dots, 8\}$, respectively. The MAS is supposed to move in an obstacle-laden environment from the initial (reference) configuration, shown in Fig. 2(a), to the target configuration shown in Fig. 2(b). UGVs are assumed to have the same size and characteristics: $\epsilon = \epsilon_i = 0.25$, $\delta = \delta_i = 1m$, for every $i \in \mathcal{V}$, and $\beta = \beta_1 = \beta_2 = 0.05$. Given UGVs' reference (initial) formation, Eq. (39) is used and $\lambda_{\min} = 0.7217$ is obtained. We constrain UGVs to remain inside the containment ball $\mathcal{B}(t)$ with constant $r_{\max} = 40$ m at any time t. This requirement is satisfied by assigning $\lambda_{\max} = 1.2917$ using Eq. (41). Therefore, it is necessary that eigenvalues of the matrix $\mathbf{U}_D(t) = \left(\mathbf{Q}^T(t)\mathbf{Q}(t)\right)$ satisfy the following safety constraints at any time t: $0.7217 \leq \lambda_i(t) \leq 1.2917,\ i = 1, 2$.

Fig. 2(c) plots the paths of all agents (shown by blue) and the center of the containment ball $\mathcal{B}$ (shown by red), from the initial configuration to the target destination. Continuum deformation coordination is simulated under two different inter-agent communication protocols shown in Fig. 2(d, e). Under the communication topology defined by graph $\mathcal{G}_1$, every follower directly accesses position information of the three leaders, thus $\mathcal{N}_i = \{1, 2, 3\}$ for every agent $i \in \mathcal{V}$. Under the communication topology defined by graph $\mathcal{G}_2$, each follower communicates with three in-neighbor agents shown in Fig. 2(e) where $w_{i,j} = \frac{1}{3}$ for every follower UGV $i \in \mathcal{V}_F$ and every in-neighbor agent $j \in \mathcal{N}_i$.

In Fig. 3(a, b), $\|\mathbf{r}_i - \mathbf{r}_{i,HT}\|$ is plotted versus time for UGVs 1 through 8. It is shown that deviation of every UGV does not $\delta = 1m$. Also, $\|\mathbf{r}_i(t_k) - \mathbf{r}_{i,HT}(t_k)\| \leq 0.05\delta$ for $k = 1, \dots, 21$ ($n_w = 21$), where $\beta = 0.05$. It is observed that safety conditions (15a) and (17) are both satisfied when MAS applies graph $\mathcal{G}_1$ or graph $\mathcal{G}_2$ to acquire the desired coordination. Fig. 3(c) plots travel intervals T_1 through T_{20} under communication graphs $\mathcal{G}_1$ or graph $\mathcal{G}_2$. Note that the total travel time under communication topology $\mathcal{G}_1$ ($t_{21} - t_1 = 491.17$ s) is smaller than the total travel time under communication topology $\mathcal{G}_2$ ($t_{21} - t_1 = 763.38$ s), respectively.

6. Conclusion and discussion

This paper proposed an approach to planning a decentralized homogeneous deformation coordination of an MAS in an obstacle laden environment. We use the A* search to assign the optimal path of the center of the containment ball $\mathcal{B}$, assuring collision avoidance of the MAS with obstacles, while the follower containment and inter-agent collision avoidance are independently planned and ensured by using the underlying principles of continuum mechanics. The proposed A*-based planning, is much faster than the one used in Rastgoftar et al. (2021) to assign the optimal paths of leaders and assures (i) obstacle collision avoidance, (ii) inter-agent collision avoidance, and (iii) follower containment through constraining the eigenvalues of the matrix $\mathbf{U}_D(t) = \left(\mathbf{Q}^T\mathbf{Q}\right)^T$ in every single search. While spatial planning of continuum deformation was completed in 8.01 seconds in this paper, Rastgoftar et al. (2021) need at least 10 minutes to spatially plan the leaders' paths optimizing a continuum deformation coordination in an obstacle-laden environment. Furthermore, the entire (spatial and temporal) continuum deformation planning was completed is 65.30 seconds. Note that the proposed temporal planning approach also speeds up the continuum deformation planning since the generalized coordinate η_k is independently determined over the time-interval $[t_k, t_{k+1}]$ for every $k = 1, \dots, n_w - 1$. Compared to Rastgoftar et al. (2021), Rastgoftar

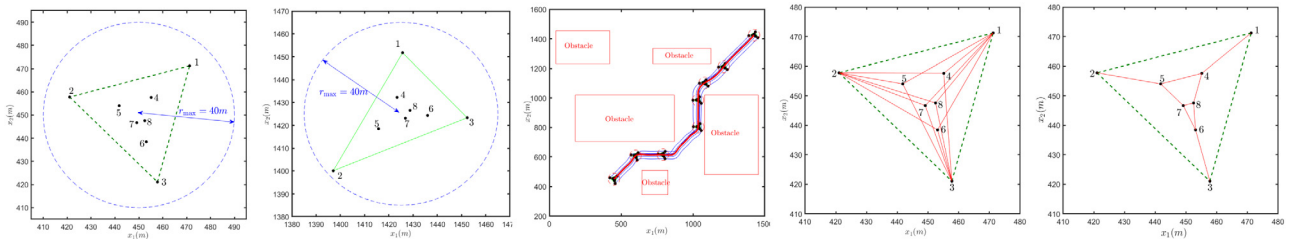

(a) Initial formation (b) Final formation (c) UGV Paths (d) Graph $\mathcal{G}_1$ (e) Graph $\mathcal{G}_2$

Fig. 2. (a, b) MAS initial and final formations enclosed by containment ball with radius $r_{\max} = 40$ m. (c) UGVs' paths (shown by blue) and path of the center of the containment ball (shown by red) from initial positions to target destinations. (d, e) Graphs $\mathcal{G}_1$ and $\mathcal{G}_2$. (For interpretation of the references to color in this figure legend, the reader is referred to the web version of this article.)

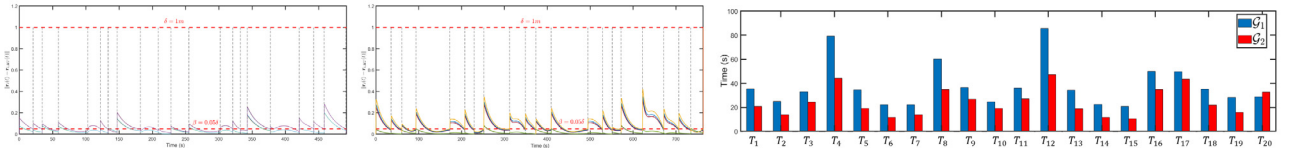

(a) (b) (c)

Fig. 3. Deviation of every UGV $i \in \mathcal{V} = \{1, \ldots, 8\}$ versus time t under (a) communication protocol defined by graph $\mathcal{G}_1(\mathcal{V}, \mathcal{E}_1)$ and (b) communication protocol defined by graph $\mathcal{G}_2(\mathcal{V}, \mathcal{E}_2)$. (c) Optimal travel intervals T_1^* through $T_{n_w^*}$ $(n_w = 21)$ under communication protocols $\mathcal{G}_1$ and $\mathcal{G}_2$.

and Kolmanovsky (2021), our proposed approach also speeds up the continuum deformation coordination, since the agents are not required to fully stop at the intermediate configurations obtained by integration of the A* search and eigen-decomposition of the homogeneous transformation coordination.

References

Al Tair, H., Taha, T., Al-Qutayri, M., & Dias, J. (2015). Decentralized multi-agent POMDPs framework for humans-robots teamwork coordination in search and rescue. In *2015 int. conf. on inf. and com. tech. research* (pp. 210–213). IEEE.

De Badyn, M. H., Eren, U., Açikmeşe, B., & Mesbahi, M. (2018). Optimal mass transport and kernel density estimation for state-dependent networked dynamic systems. In *2018 IEEE conference on decision and control* (pp. 1225–1230). IEEE.

Dibaji, S. M., & Ishii, H. (2017). Resilient consensus of second-order agent networks: Asynchronous update rules with delays. *Automatica*, *81*, 123–132.

Ji, M., Ferrari-Trecate, G., Egerstedt, M., & Buffa, A. (2008). Containment control in mobile networks. *IEEE Transactions on Automatic Control*, *53*(8), 1972–1975.

Klausen, K., Fossen, T. I., Johansen, T. A., & Aguiar, A. P. (2015). Cooperative path-following for multirotor uavs with a suspended payload. In *2015 IEEE conference on control applications* (pp. 1354–1360). IEEE.

Li, B., Chen, Z.-q., Liu, Z.-x., Zhang, C.-y., & Zhang, Q. (2016). Cont. cont. of multi-agent sys. with fixed time-delays in fixed directed networks. *Neurocomputing*, *173*, 2069–2075.

Li, N. H., & Liu, H. H. (2008). Formation UAV flight control using virtual structure and motion synchronization. In *2008 american control conference* (pp. 1782–1787). IEEE.

Li, Y., Tang, C., Li, K., Peeta, S., He, X., & Wang, Y. (2018). Nonlinear finite-time consensus-based connected vehicle platoon control under fixed and switching communication topologies. *Transportation Research Part C (Emerging Technologies)*, *93*, 525–543.

Lin, X., & Zheng, Y. (2016). Finite-time consensus of switched multiagent systems. *IEEE Transactions on Systems, Man, and Cybernetics: Systems*, *47*(7), 1535–1545.

Liu, H., Cheng, L., Tan, M., & Hou, Z.-G. (2015). Containment control of continuous-time linear multi-agent systems with aperiodic sampling. *Automatica*, *57*, 78–84.

Liu, H., Cheng, L., Tan, M., & Hou, Z.-G. (2018). Exponential finite-time consensus of fractional-order multiagent systems. *IEEE Transactions on Systems, Man, and Cybernetics: Systems*.

Rastgoftar, H. (2020). Fault-resilient continuum deformation coordination. *IEEE Transactions on Control of Network Systems*.

Rastgoftar, H., Atkins, E. M., & Kolmanovsky, I. V. (2021). Scalable vehicle team continuum deformation coordination with eigen decomposition. *IEEE Transactions on Automatic Control*, 1.

Rastgoftar, H., & Kolmanovsky, I. V. (2021). Safe affine transformation-based guidance of a large-scale multi-quadcopter system (MQS). *IEEE Transactions on Control of Network Systems*.

Rastgoftar, H., Zhang, B., & Atkins, E. M. (2018). A data-driven approach for autonomous motion planning and control in off-road driving scenarios. In *2018 american control conference* (pp. 5876–5883). IEEE.

Remagnino, P., Tan, T., & Baker, K. (1998). Multi-agent visual surveillance of dynamic scenes. *Image and Vision Computing*, *16*(8), 529–532.

Shang, Y. (2018). Resilient consensus of switched multi-agent systems. *Systems & Control Letters*, *122*, 12–18.

Tseng, F. H., Liang, T. T., Lee, C. H., Der Chou, L., & Chao, H. C. (2014). *2014 tenth int. conf. on intel. inf. hiding and multimedia signal proc.* (pp. 942–945). IEEE.

Wang, D., & Wang, W. (2019). Necessary and sufficient conditions for containment control of multi-agent systems with time delay. *Automatica*, *103*, 418–423.

Zhai, C., & Hong, Y. (2013). Decentralized sweep coverage algorithm for multi-agent systems with workload uncertainties. *Automatica*, *49*(7), 2154–2159.

Zhao, Y., & Duan, Z. (2015). Finite-time containment control without velocity and acceleration measurements. *Nonlinear Dynamics*, *82*(1–2), 259–268.

Zhao, Y.-P., He, P., Saberi Nik, H., & Ren, J. (2015). Robust adaptive synchronization of uncertain complex networks with multiple time-varying coupled delays. *Complexity*, *20*(6), 62–73.

Zhou, J., Sang, C., Li, X., Fang, M., & Wang, Z. (2018). H consensus for nonlinear stochastic multi-agent systems with time delay. *Applied Mathematics and Computation*, *325*, 41–58.

Hossein Rastgoftar is an Assistant Professor in the Department of Aerospace and Mechanical Engineering at the University of Arizona. He received the B.Sc. degree in mechanical from Shiraz University, Shiraz, Iran, the M.S. degrees in mechanical systems and solid mechanics from Shiraz University and the University of Central Florida, Orlando, FL, USA, and the Ph.D. degree in mechanical engineering from Drexel University, Philadelphia, in 2015.

Ilya V. Kolmanovsky received M.S. and Ph.D. degrees in aerospace engineering and the M.A. degree in mathematics from the University of Michigan, Ann Arbor, MI, USA, in 1993, 1995, and 1995, respectively. He is currently a Professor with the Department of Aerospace Engineering, University of Michigan. His research interests include control theory for systems with state and control constraints, and control applications to aerospace and automotive systems.